

# Synthesis and characterization of a disubstituted piperazine derivative with T-type channel blocking action and analgesic properties

Zubaidha Pudukulatham, PhD<sup>1</sup>, Fang-Xiong Zhang, PhD<sup>2,3</sup>, Vinicius M Gadotti, PhD<sup>2,3</sup>, Said M'Dahoma, PhD<sup>2,3</sup>, Prabhuling Swami, MSc<sup>1</sup>, Yasinalli Tamboli, PhD<sup>1</sup> and Gerald W Zamponi, PhD<sup>2,3</sup>

## Abstract

**Background:** T-type calcium channels are important contributors to signaling in the primary afferent pain pathway and are thus important targets for the development of analgesics. It has been previously reported that certain piperazine-based compounds such as flunarizine are able to inhibit T-type calcium channels. Thus, we hypothesized that novel piperazine compounds could potentially act as analgesics.

**Results:** Here, we have created a series of 14 compound derivatives around a diphenyl methyl-piperazine core pharmacophore. Testing their effects on transiently expressed Cav3.2 calcium channels revealed one derivative (3-((4-(bis(4-fluorophenyl)methyl)piperazin-1-yl)methyl)-4-(2-methoxyphenyl)-1,2,5-oxadiazole 2-oxide, compound 10e) as a potent blocker. 10e mediate tonic block of these channels with an IC<sub>50</sub> of around 4 micromolar. 10e also blocked Cav3.1 and Cav3.3 channels, but only weakly affected high-voltage-activated Cav1.2 and Cav2.2 channels. Intrathecal delivery of 10e mediated relief from formalin and complete Freund's adjuvant induced inflammatory pain that was ablated by genetic knockout of Cav3.2 channels.

**Conclusions:** Altogether, our data identify a novel T-type calcium channel blocker with tight structure activity relationship (SAR) and relevant in vivo efficacy in inflammatory pain conditions.

## Keywords

T-type, pain, calcium channel, piperazine, analgesia

Date received: 16 December 2015; revised: 14 January 2016; accepted: 27 January 2016

## Introduction

Voltage-gated calcium channels are a major contributor to depolarization-mediated calcium influx into electrically excitable cells where they fulfill a plethora of physiological functions including neurotransmitter release, muscle contraction, and pace making.<sup>1,2</sup> The voltage-gated calcium channel family includes three different types of T-type calcium channels (Cav3.1, Cav3.2, and Cav3.3),<sup>3</sup> which, by virtue of their unique biophysical characteristics, are ideally suited toward regulating neuronal excitability and low-threshold exocytosis.<sup>4,5</sup> Their dysfunction has been associated with the occurrence of absence of seizures<sup>6,7</sup> and pain hypersensitivity.<sup>8</sup> In particular, the Cav3.2 calcium channel subtype appears to be the main isoform

involved in peripheral pain signaling,<sup>8</sup> and Cav3.2 channels are upregulated in primary afferent fibers in various chronic pain conditions.<sup>9–11</sup> Consequently, these channels

<sup>1</sup>School of Chemical Sciences, SRTM University, Nanded, Maharashtra, India

<sup>2</sup>Department of Physiology and Pharmacology, Cumming School of Medicine, University of Calgary, Calgary, Alberta, Canada

<sup>3</sup>Alberta Children's Hospital Research Institute, University of Calgary, Calgary, Alberta, Canada

### Corresponding author:

Gerald W Zamponi, University of Calgary Cumming School of Medicine, 3330 Hopsital Dr NW, Calgary, Alberta T2N 4N1, Canada.

Email: zamponi@ucalgary.ca



are considered important pharmacological targets.<sup>2,12</sup> Several classes of T-type calcium channel blocking molecules have been identified and shown to mediate analgesic effects in rodent models of inflammatory and neuropathic pain,<sup>13–16</sup> but none of these compounds have so far passed clinical trials.<sup>17</sup> Hence, identifying potent T-type calcium channel blockers with clinical efficacy as analgesics remains highly desirable.

A majority of bioactive molecules are heterocyclic compounds. Piperazine and its derivatives have played a significant role in medicinal chemistry. Piperazine is a small molecule with a rigid backbone with numerous biological activities such as anticancer,<sup>18,19</sup> calcium channel blockers,<sup>20,21</sup> antimalarial,<sup>22</sup> antihistamine,<sup>23,24</sup> antimicrobial,<sup>25</sup> antidepressant,<sup>26</sup> antioxidant,<sup>27</sup> antiallergic,<sup>28</sup> antiviral,<sup>29</sup> antipsychotic,<sup>30</sup> and antiparasitic<sup>31,32</sup> activity. The various biological activities of piperazine nuclei are due to easy modification, proper alkalinity, water solubility, capacity for formation of hydrogen bonds, and adjustment of molecular physicochemical properties.<sup>33</sup> We report herein the synthesis of 14 new disubstituted piperazine derivatives (Figures 1 and 2) and their further biological evaluation. We identify a novel T-type calcium channel inhibitor with potent analgesic effects in a mouse model of inflammatory pain.

## Methods

### Cell culture and transient transfection

Human embryonic kidney cells (HEK) tsA-201 cells were grown to 80–90% confluence at 37°C (5% CO<sub>2</sub>) in Dulbecco's modified Eagle's medium (Life Technologies, Grand Island, NY), supplemented with 10% (vol/vol)

fetal bovine serum (HyClone, Thermo Scientific, Pittsburgh, PA), 200 U/ml penicillin, and 0.2 mg/ml streptomycin (Life Technologies, Grand Island, NY). Cells were suspended with 0.25% trypsin/ethylenediaminetetraacetic acid and plated onto glass coverslips in 10-cm culture dishes (Corning, Corning, NY) at 10% confluence 6 h before transfection. Calcium channel (5 μg) and green fluorescent protein (GFP) marker (0.5 μg) DNAs were transfected into cells with calcium phosphate. For Cav1.2 and Cav2.2, the additional Cavβ1 b (5 μg) and Cavα2δ1 (5 μg) subunits were coexpressed. Cells were transferred to 30°C 16–18 h later following transfection and stored for two days before recording.

### Electrophysiology

Cells on a glass coverslip were transferred into an external bath solution of 20 mM BaCl<sub>2</sub>, 1 mM MgCl<sub>2</sub>, 40 mM TEACl, 65 mM CsCl, 10 mM HEPES, and 10 mM glucose, pH 7.4. Borosilicate glass pipettes (Sutter Instrument Co., Novato, CA; 3–5 MΩ) were filled with internal solution containing 140 mM CsCl, 2.5 mM CaCl<sub>2</sub>, 1 mM MgCl<sub>2</sub>, 5 mM EGTA, 10 mM HEPES, 2 mM Na-ATP, and 0.3 mM Na-GTP, pH 7.3. Whole-cell patch clamp recordings were performed by using an EPC 10 amplifier (HEKA Elektronik, Bellmore, NY) linked to a personal computer equipped with Pulse (V8.65) software (HEKA Elektronik). After seal formation, the membrane beneath the pipette was ruptured and the pipette solution was allowed to dialyze into the cell for 2–5 min before recording. Voltage-dependent currents were leak corrected with an online P/4 subtraction paradigm. Data were recorded at 10 kHz and filtered

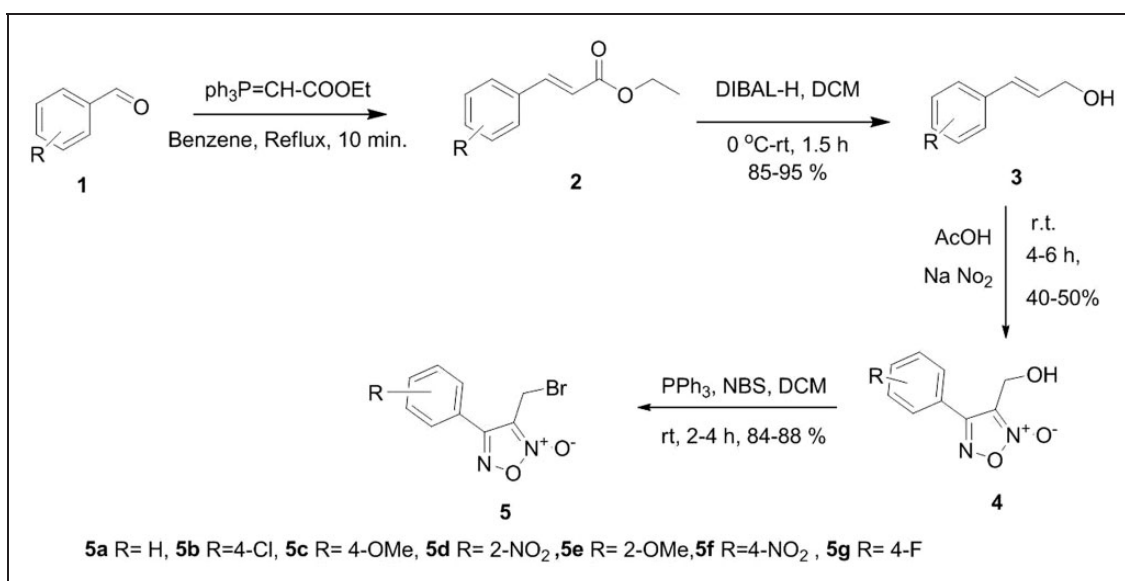


**Figure 1.** Synthesis of substituted bromo furoxan.

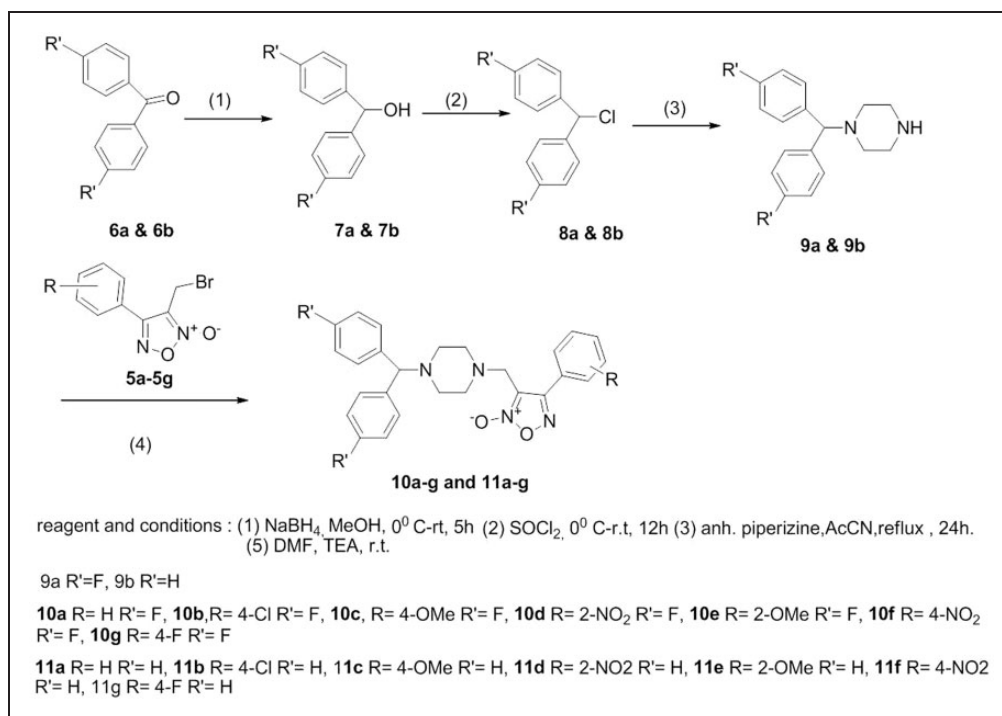


**Figure 2.** Synthesis of disubstituted piperazine derivatives.

at 2.9 kHz. T-type calcium currents were elicited by depolarization from a holding potential of  $-110\text{ mV}$  to a test potential of  $-20\text{ mV}$  and N-type or L-type calcium currents were elicited by depolarization from a holding potential of  $-90\text{ mV}$  to a test potential of  $+20\text{ mV}$ , with an interpulse interval of 20 s. The duration of the test pulse was typically 100 ms. In current-voltage relation studies for Cav3.2, the membrane potential was held at  $-110\text{ mV}$  and cells were depolarized from  $-60$  to  $+60\text{ mV}$  in 5 mV increments. In steady-state inactivation studies for Cav3.2, a 3 s conditioning prepulse of various magnitudes (initial holding at  $-110\text{ mV}$ ) was followed by a depolarizing pulse to  $-20\text{ mV}$ . Individual sweeps were separated by 12 s to permit recovery from inactivation between conditioning pulses. The current amplitude obtained from test pulse was normalized to that observed at the holding potential of  $-110\text{ mV}$ .

### Animals

Experiments were performed after approval of the animal protocol by the Institutional Animal Care and Use Committee and best efforts were made to minimize animal suffering and distress according to the policies and recommendations of the International Association for the Study of Pain. Adult male C57BL/6 J (wild-type) or CACNA1H knockout (Cav3.2 null) mice (20–25 g) were used and housed at a maximum of five per cage ( $30 \times 20 \times 15\text{ cm}$ ) with free access to food and water. Animals were kept in controlled temperature of

$23 \pm 1^\circ\text{C}$  on a 12 h light/dark cycle (lights on at 7:00 a.m.). When drugs were delivered by the intrathecal (i.t.) route, a volume of  $10\ \mu\text{l}$  was injected to conscious mice as described previously by our laboratory.<sup>15,34</sup> All drugs were dissolved in dimethyl sulfoxide (DMSO) and control animals received phosphate-buffered saline (PBS) + DMSO 1%, which was the maximum DMSO concentration in solutions delivered to animals. Wild type and Cav3.2 null mice (Homozygous CACNA1H) were purchased from Jackson Laboratories and different cohorts of mice were used for each test and each mouse was used only once. The observer was blind to the experimental conditions in the experiment examining the action of compound 10e on complete Freund's adjuvant (CFA)-induced persistent pain.

### Formalin test

Mice were allowed to acclimatize to the laboratory for at least 60 min before beginning of experiments. Each mouse received  $20\ \mu\text{l}$  of a formalin solution (1.25%, in PBS) injected in the ventral surface of the right hind paw (intraplantarily, i.pl.). Following i.pl. injections of formalin, animals were placed individually into observation chambers and observed individually between 0–5 min (acute tonic phase) and 15–30 min (acute inflammatory phase). The time animals spent licking or biting the paw injected with formalin was scored with a chronometer and considered as nocifensive response.<sup>37</sup>

## Persistent inflammatory pain induced by CFA

To induce mechanical hyperalgesia caused by peripheral inflammation, animals received 20  $\mu$ l of CFA injected i.pl. in the right hind paw.<sup>38</sup> Sham groups received 20  $\mu$ l of PBS in the ipsilateral paw. Animals were treated with either compound 10e (0.03–10  $\mu$ g/i.t.) or vehicle (10  $\mu$ l/i.t.) two days following CFA injection and their mechanical withdrawal threshold was subsequently tested.

## Evaluation of mechanical hyperalgesia

Mechanical hyperalgesia was measured by the use of a Dynamic Plantar Aesthesiometer (DPA, Ugo Basile, Varese, Italy). Mice were placed individually in small enclosed testing arenas (20 cm  $\times$  18.5 cm  $\times$  13 cm, length  $\times$  width  $\times$  height) on top of a wire grid platform. Mice were allowed to acclimate for at least 90 min before the baselines were taken. The DPA device was manually positioned beneath the animal before each measurement, so that the filament was directly under the plantar surface of the ipsilateral hind paw. Each paw was tested three times per session.

## Data analysis and statistics

Data analysis was performed by using online analysis built in Pulse software (HEKA Elektronik), and all graphs and curve fittings were prepared by using GraphPad Prism 5 (GraphPad Software, La Jolla, CA). Dose–response curves were fitted with the equation  $y = A_2 + (A_1 - A_2)/(1 + ([C]/IC_{50})^n)$ , where  $A_1$  is initial current amplitude and  $A_2$  is the current amplitude at saturating drug concentrations,  $[C]$  is the drug concentration, and  $n$  is the Hill coefficient. Current–voltage relationships were fitted with the modified Boltzmann equation:  $I = [G_{max}(V_m - E_{rev})]/[1 + \exp((V_{0.5act} - V_m)/\kappa_a)]$ , where  $V_m$  is the test potential,  $V_{0.5act}$  is the half activation potential,  $E_{rev}$  is the reversal potential,  $G_{max}$  is the maximum slope conductance, and  $\kappa_a$  reflects the slope of the activation curve. Steady-state inactivation curves were fitted using the Boltzmann equation:  $I = 1/(1 + \exp((V_m - V_h)/\kappa))$ , where  $V_h$  is the half-inactivation potential and  $\kappa$  is the slope factor. Statistical significance was determined by paired or unpaired Student's  $t$  tests. Significance values were set as indicated in the text and figure legends. All data are given as mean values  $\pm$  standard errors.

## Chemical analysis

Melting points were determined using the open capillary method and are uncorrected. <sup>1</sup>H NMR and <sup>13</sup>C NMR spectra were recorded on either a Bruker Avance 300 MHz or a Varian Inova 400 and 500 MHz FT

spectrometer using TMS as an internal standard (chemical shift in  $\delta$  values,  $J$  in Hz). High resolution mass spectra and electrospray ionization recorded on QSTAR XL High resolution mass spectrometer. All reagents and solvents used are commercially available. Column chromatography was performed using silica gel (60–120 mesh).

## General synthesis strategy

Bromo Furoxan derivatives (5a–5g) were obtained from cinnamyl alcohol (3a–3g) in good yield as shown in Figure 1. Substituted benzaldehydes were treated with witting reagent to give cinnamates (2a–2g), which were reduced to corresponding cinnamyl alcohol using diisobutylaluminium hydride (DIBAL-H). Furoxan alcohols (4a–4g) were obtained from cinnamyl alcohol using sodium nitrite/acetic acid. An Appel reaction of furoxan alcohol using *N*-bromosuccinimide (NBS)/triphenylphosphine (PPh<sub>3</sub>) was used to obtain corresponding bromo furoxan in good yield (5a–5g). 1-Benzhydrylpiperazine and 4,4-difluoro-1-benzhydrylpiperazine were prepared as shown in Figure 2. Reduction of benzophenones (6a–6b) by sodium borohydride provided benzhydryl compounds (7a–7b) in high yield (90%). Subsequently, these benzhydryl derivatives were treated with thionyl chloride at ambient temperature to give corresponding benzhydryl chloride (8a–8b). Treatment of these chlorides with piperazine and anhydrous potassium carbonate furnished key intermediate benzhydrylpiperazines (9a–9b). Nucleophilic substitution reaction of benzhydrylpiperazine with different furoxan bromides (5a–5g) was used to produce final furoxan-coupled piperazine products (10a-g and 11a-g) with excellent yields (Figure 2).

## Synthesis of substituted ethyl cinnamate

To a solution of benzaldehyde (2 g) in benzene (20 ml) under reflux condition was added C<sub>2</sub>-wittig reagent and allowed to stir for 10 min. The progress of reaction was monitored by thin-layer chromatography (TLC). After completion of reaction, it was quenched by water. The reaction mixture was extracted by chloroform (2  $\times$  10 ml) and concentrated under reduced pressure to give the crude product. The crude residue was purified on silica gel column chromatography. Yield: 2.5 g (80%)

## General Procedure for syntheses of substituted cinnamyl alcohols

To a solution of the corresponding cinnamate (10 mmol) in dichloromethane (DCM; 25 ml), DIBAL (22 mmol, 25 % in toluene) was added dropwise over 30 min at 0°C. The reaction mixture was allowed to warm to room

temperature and stirred for 1 h. The reaction mixture was quenched with saturated solution of sodium potassium tartrate. The organic layer was separated and the aqueous layer was extracted with chloroform. The combined organic layer was washed with brine and water, dried ( $\text{Na}_2\text{SO}_4$ ), filtered, and concentrated under reduced pressure. The crude residue was purified on silica gel column chromatography. Gradient elution with ethyl acetate (20–40%) in hexane yielded the product.

#### Synthesis of substituted 3-(hydroxymethyl)-4-phenyl-1,2,5-oxadiazole 2-oxide

To a solution of cinnamyl alcohol (1 mmol) in glacial acetic acid (5 ml) was added saturated sodium nitrite solution (10–20 mmol for deactivated aryl groups and 4 mmol for activated aryl groups) portion wise over 45 min. The reaction mixture was stirred at room temperature for 4–8 h. After completion of the reaction, the reaction mixture was quenched with ice water and extracted with ethyl acetate. The ethyl acetate layer was washed successively with saturated  $\text{NaHCO}_3$ , water, brine then dried ( $\text{Na}_2\text{SO}_4$ ) and concentrated under reduced pressure to give the crude product. The crude residue was purified on silica gel column chromatography. Gradient elution with ethyl acetate (10–40%) in hexane yielded the product.

#### Synthesis of substituted 3-(bromomethyl)-4-phenyl-1,2,5-oxadiazole 2-oxide

To the solution of alcohol compound (0.5 g, 2.38 mmol) and  $\text{PPh}_3$  (0.96 g, 4.76 mmol) in DCM (20 ml), NBS (0.63 g, 3.57 mmol) was added portion wise over a period of 30 min. The reaction mixture was stirred for an additional 2 h. The progress of reaction was monitored by TLC. After completion of reaction, the reaction mixture was quenched with ice water and extracted with chloroform ( $2 \times 10$  ml) and concentrated under reduced pressure to give the crude product. The crude residue was purified on silica gel column chromatography. Gradient elution with ethyl acetate (5–10%) in hexane yielded the product.

#### Procedure for synthesis of substituted furoxan coupled piperazine derivatives

To the stirred solution of substituted benzhydryl piperazine (1 mmol) and triethyl amine (2 mmol) in dimethylformamide (3 ml), substituted 3-(bromomethyl)-4-phenyl-1,2,5-oxadiazole 2-oxide (1 mmol) was added and stirred at room temperature. After completion of reaction monitored by TLC, ice cold water was added to the reaction mixture and allowed to stir for 10 min. The reaction mixture was extracted with ethyl

acetate and washed with cold water. The organic layer was dried over  $\text{Na}_2\text{SO}_4$  and concentrated under reduced pressure to obtain the crude product, which was purified by column chromatography over silica gel (60–120 mesh) using hexane:ethyl acetate as eluent.

## Results

### Electrophysiological analysis of Cav3.2 channel block

The blocking effects of all 14 benzhydryl piperazine derivatives (10a–10g and 11a–11g) were tested on transiently expressed the T-type calcium channels-Cav3.2 at a concentration of  $10 \mu\text{M}$  using whole-cell patch clamp recording. As shown in Figure 3(a), only compound

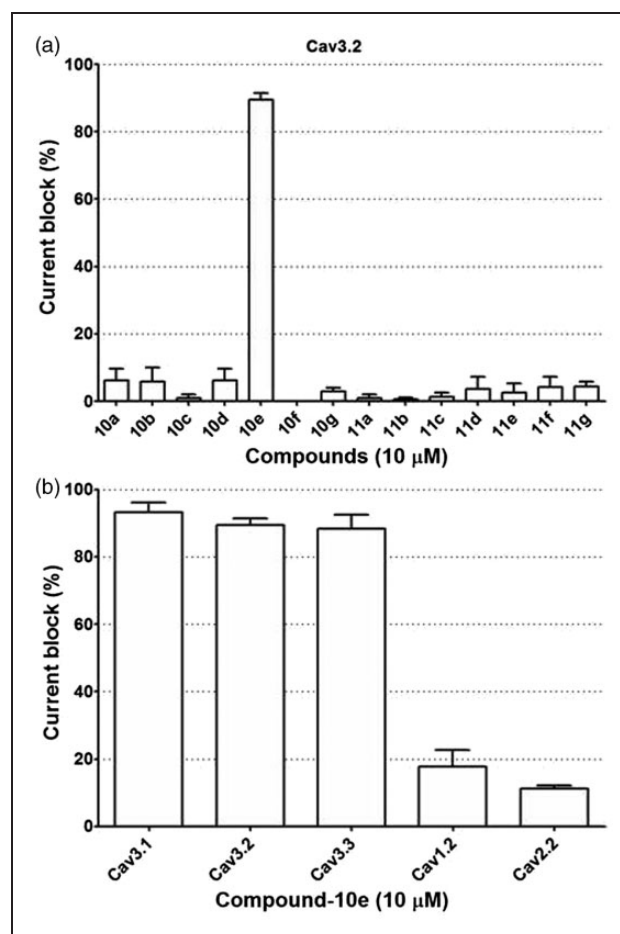


**Figure 3.** (a) Percentage of whole cell current inhibition of Cav3.2 (T-type) in response to  $10 \mu\text{M}$  application of the compound series ( $n = 3$  per compound). Note the effective block of Cav3.2 by compound 10 e. (b) Percentage of whole cell current inhibition of Cav3.1 (T-type), Cav3.2 (T-type), Cav3.3 (T-type), Cav1.2 (L-type), and Cav2.2 (N-type) in response to  $10 \mu\text{M}$  application of compound 10 e ( $n = 3$  per channel). Note the selective block of all the T-type calcium channels by compound 10 e.

10e effectively blocked Cav3.2 channels with  $89.46 \pm 1.96\%$  inhibition. The remaining 13 compounds mediated only minor effects on Cav3.2 channels, with inhibition ranging from 0.0 to 6.29% (Figure 3a). Interestingly, 10e also blocked the other two T-type calcium channel isoforms (Cav3.1 and Cav3.3) with similar potency ( $93.30 \pm 2.78\%$  inhibition and  $88.41 \pm 4.08\%$  inhibition, respectively). The compound failed to effectively block L-type (Cav1.2;  $17.82 \pm 4.79\%$  inhibition) and N-type (Cav2.2;  $11.21 \pm 0.86\%$  inhibition) currents (Figure 3b). Taken together, compound 10e is an effective and preferential blocker of T-type calcium channels (Cav3.2, Cav3.1, and Cav3.3) over Cav1.2 and Cav2.2.

Next, we assessed dose dependence and biophysical characteristics of compound 10e block of Cav3.2. The  $IC_{50}$  of compound 10e determined from the fitted dose-response curve was  $3.80 \pm 0.30 \mu\text{M}$  (Figure 4a). Compound 10e had no significant effects on half-

activation potential ( $p = 0.72$ , Figure 4b) and half-inactivation potential of Cav3.2 ( $p = 0.12$ , Figure 4c), indicating that this compound is a tonic rather than a state-dependent blocker.

### Effect of compound 10e on biphasic acute pain

Given the blocking activity on T-type channels, we hypothesized that this compound could protect against pain in animal models. Compound 10e was delivered by the i.t. route and its effects on both the tonic nociceptive and the later acute inflammatory pain phases of the formalin test were evaluated. Animals were injected intrathecally with increasing doses of compound 10e or yet with control vehicle (PBS + DMSO 1%) 20 min before formalin injection. One-way analysis of variance (ANOVA) revealed that i.t. treatment of mice with compound 10e ( $0.03\text{--}0.3 \mu\text{g}/\text{i.t.}$  significantly reduced

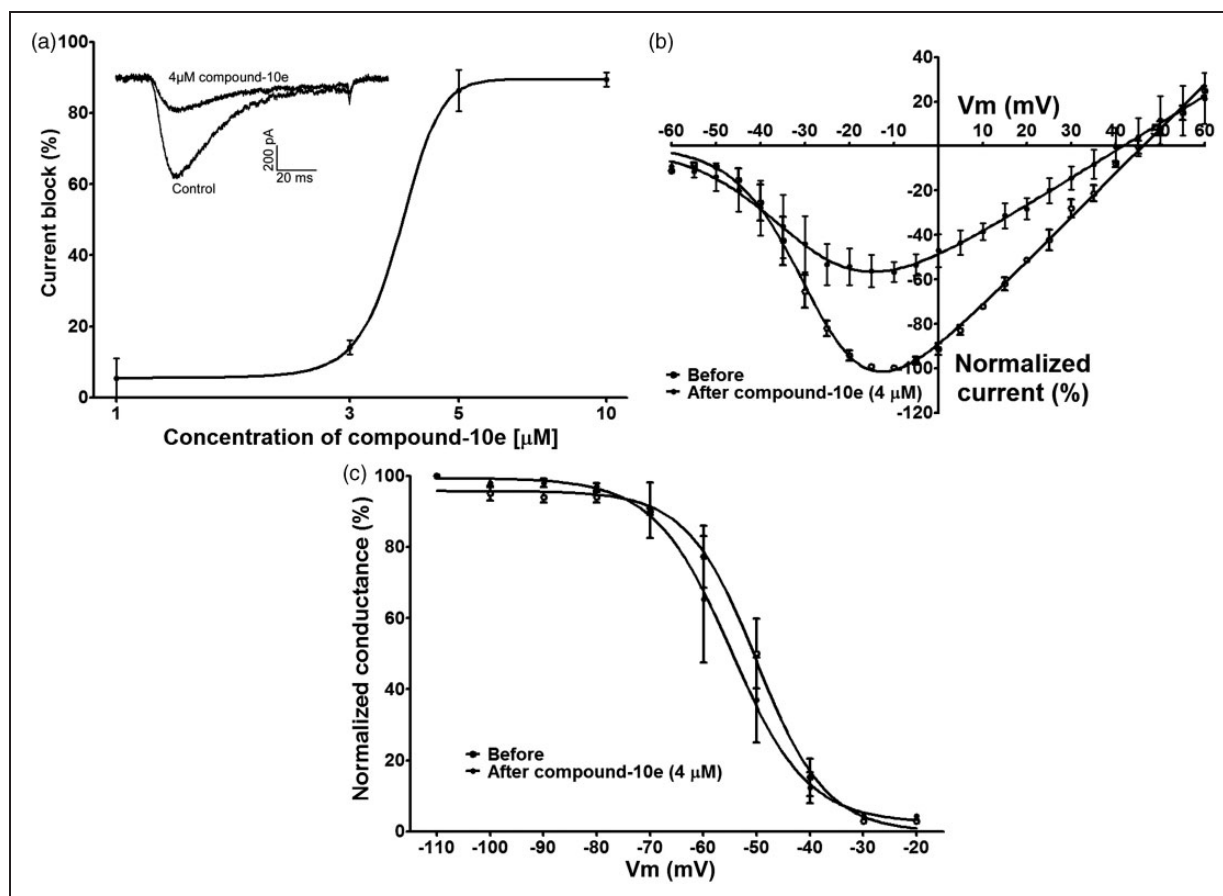


**Figure 4.** (a) Dose-response relation for compound 10 e block of Cav3.2. The  $IC_{50}$  from the fitted curve was  $3.80 \pm 0.30 \mu\text{M}$  ( $n = 3$  per dose). The inset shows a representative T-type current in the presence and the absence of  $4 \mu\text{M}$  of compound 10 e. The test potential was  $-20 \text{ mV}$ . (b) Current-voltage relation for compound 10 e block of Cav3.2. The half-activation potential from the fitted curves were  $-27.30 \pm 0.61 \text{ mV}$  and  $-30.19 \pm 2.62 \text{ mV}$  for before and after the application of compound 10 e ( $4 \mu\text{M}$ ,  $n = 3$ ),  $p = 0.72$  (paired  $t$  test). (c) The steady-state inactivation curve for compound 10 e block of Cav3.2. The half-inactivation potential from the fitted curves were  $-50.00 \pm 1.20$  and  $54.86 \pm 1.92 \text{ mV}$  for before and after the application of compound 10 e ( $4 \mu\text{M}$ ,  $n = 3$ ),  $p = 0.12$  (paired  $t$  test).

nocifensive responses of mice time in both first (Figure 5a) and second (Figure 5b) phases ( $38 \pm 4\%$  and  $48 \pm 12\%$  inhibition, respectively).

To verify whether the effects observed for compound 10e were indeed mediated by T-type channels, we repeated the formalin test in Cav3.2 null mice and wild-type animals. As shown in Figure 5(c) and 5(d), compound 10e lacks analgesic activity in both phases of formalin test when delivered to Cav3.2 null mice, thus suggesting that Cav3.2 channels mediate the analgesic action observed for compound 10e.

### Effect of compound 10e on persistent peripheral inflammatory pain

To verify whether compound 10e is also efficacious against persistent inflammatory pain, we analyzed mechanical hypersensitivity of mice injected with CFA and treated with compound 10e. As shown in Figure 6, mice injected with CFA developed mechanical hyperalgesia as indicated by a decrease in paw withdrawal thresholds when compared with the pre-CFA baseline levels of the vehicle control group (Two-way ANOVA,

$p < 0.0001$ ). Two days following CFA injection, i.t. delivery of compound 10e at  $0.3 \mu\text{g}/\text{i.t.}$  significantly reversed mechanical hyperalgesia caused by CFA from 20 min up to 3 h ( $p < 0.001$  for  $0.3 \text{ mg}/\text{kg}$ ) relative to vehicle-treated controls (Figure 6). Altogether, these data indicate that compound 10e has analgesic properties by virtue of its T-type channel inhibition.

## Discussion

T-type calcium channels are important pharmacological targets in the treatment of absence seizures and chronic pain states.<sup>39,12</sup> Indeed, several T-type calcium channel inhibitors such as ethosuximide are used clinically to treat absence epilepsy.<sup>40</sup> Yet, only limited numbers of potent and selective T-type calcium channel antagonists that have been identified, with the most notable examples including Z944,<sup>41</sup> TTA-A2,<sup>42</sup> and TTA-P2.<sup>43</sup> In addition, a number of other T-type channel blocking pharmacophores have been identified, and compound derivatives tested in recombinant Cav3 channels.<sup>13–16</sup> To our knowledge, only two of these novel compounds have been entered into clinical trials—Z944 is currently

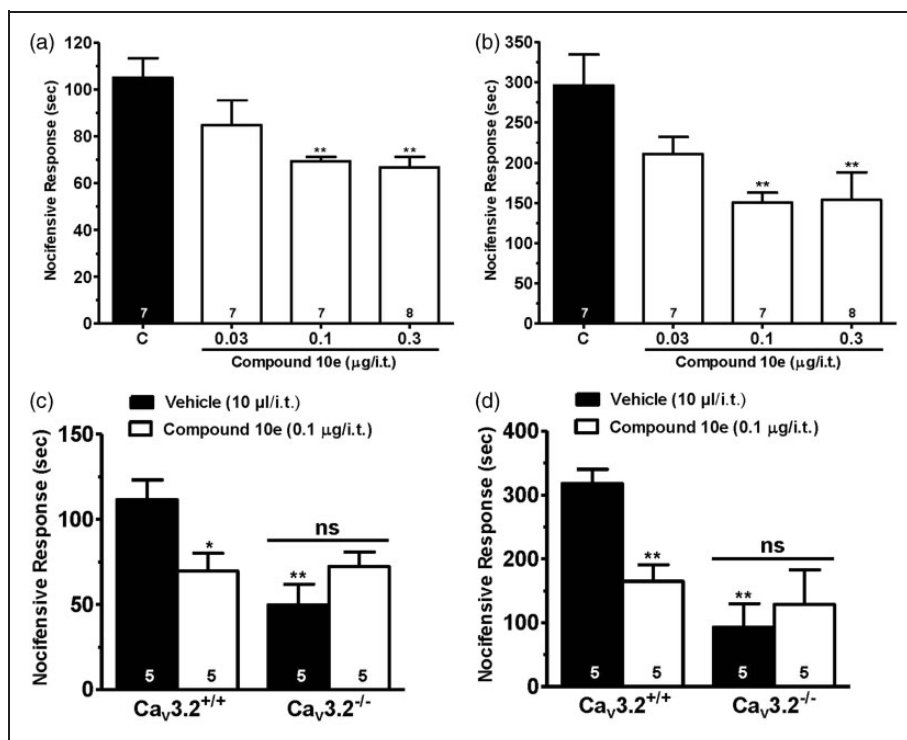


**Figure 5.** Effect of increasing doses of intrathecally delivered compound 10e on the first (a) and second (b) phases of formalin-induced pain. Comparison of effect of compound 10e ( $0.3 \mu\text{g}/\text{i.t.}$ ) on the first (c) and second (d) phases of formalin-induced pain in wild-type and Cav3.2 knockout mice, respectively. (\* $p < 0.05$ , \*\* $p < 0.01$  comparing to vehicle-treated wild-type mice, one- or two-way ANOVA, respectively for panels a, b and c, d followed by Tukey's test). Control values (indicated by "C") are from animals injected with 1% of DMSO and the asterisks denote the significance relative to the control group. Data are representative of three independent experiments. ANOVA: analysis of variance; DMSO: dimethyl sulfoxide.

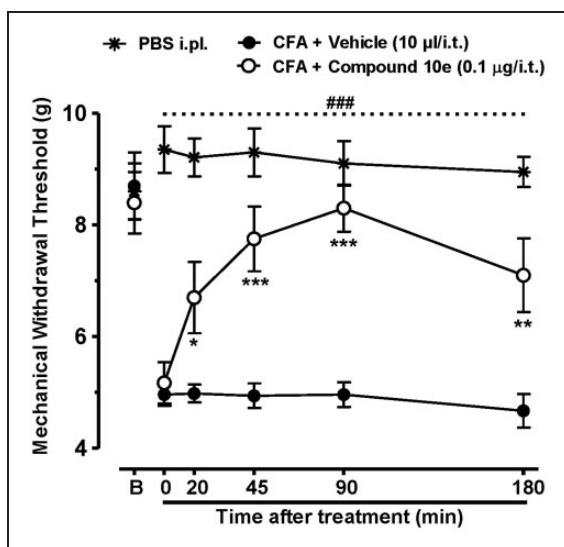


**Figure 6.** Blind analyses of the time course of analgesic action of compound 10e on persistent inflammatory pain induced by CFA. Each circle represents the mean  $\pm$  S.E.M. ( $n = 6-7$ ) and is representative of two independent experiments. (\* $p < 0.05$ , \*\* $p < 0.05$ , \*\*\* $p < 0.001$ , two-way ANOVA followed by a Tukey's test). The dashed line and hashtag indicate the range of data points where injured animals differed from the sham-treated group ( $p < 0.001$ ). CFA: complete Freund's adjuvant; ANOVA: analysis of variance.

in phase II trials for chronic pain, and ABT-639 has failed phase II clinical trials for diabetic pain.<sup>17</sup> Hence, identification of new T-type calcium channel inhibitors remains of great importance. Here, we show that disubstituted piperazine compounds have the propensity to block T-type calcium channels and that this blocking activity results in analgesic effects in a rodent model of inflammatory pain. This in turn could form the basis for the development of T-type channel inhibitors with higher affinity and perhaps with T-type channel subtype selectivity. Indeed, it has been a challenge to identify T-type channel inhibitors with selectivity among the various T-type calcium channel isoforms, although some progress has been made in this regard.<sup>41</sup>

It is remarkable that only one compound (10e) in this series mediated potent inhibition of Cav3.2 channels. A close inspection of the chemical structures of these compounds reveals insights into the structure-activity relationship. For example, compounds 10e and 11e differ only in the presence or absence of the two fluorine atoms at the diphenyl moiety, suggesting that these groups are essential determinants of Cav3.2 channel inhibition. Along these lines, compounds 10a and 10c differ from 10e in either the addition or position of the methoxy group on the single phenyl ring. Replacement of the methoxy group with a nitro group (compound 10d) eliminates activity. These data indicate that a methoxy

phenyl group in the "2" position on the phenyl ring is also essential for Cav3.2 channel block. Altogether, these data indicate that specific substituents at both ends of the benzhydryl piperazine pharmacophores are key determinants of Cav3.2 channel interactions. In this context, it is interesting to note that the nonselective T-type channel inhibitor flunarizine carries the same fluorophenyl moiety as compound 10e.<sup>44</sup> Along these lines, the structurally related diphenyl-butyl-piperidines pimozone and penfluridol potentially lock T-type channels.<sup>44</sup>

The biophysical characteristics of compound 10e indicate that there is no significant effect on the half-activation potential nor on the half-inactivation potential. Collectively, these observations suggest that this compound is not a strong state dependent inhibitor of Cav3.2 channels. This contrasts with observations concerning penfluridol and pimozone inhibition of Cav3.1 channels<sup>44</sup> and with flunarizine block of native smooth muscle T-type calcium channels which undergo drug-induced hyperpolarizing shift in the midpoint of the steady-state inactivation curve.<sup>45</sup> As the 3-((4-(bis(4-fluorophenyl)methyl)piperazine moiety in flunarizine is identical to that of compound 10e, this may indicate that state dependence is mediated by substituents on the other half of the molecule.

Compound 10e also inhibited Cav3.1 and Cav3.3 channels, but only weakly affected two members of the high-voltage-activated calcium channel family—Cav1.2 and Cav2.2, although some block of these channels was observed at a concentration of 10  $\mu$ M. Cav2.2 channels are known to be important players in the transmission of pain signals.<sup>39</sup> However, the physiological effects of compound 10e of our *in vivo* experiments can be attributed exclusively to an action on Cav3.2 channels, as the analgesic effects were ablated in Cav3.2 channel knockout mice. We did not observe any noticeable side effects; however, it is important to note that the compound was delivered intrathecally, which biases action toward the primary afferent pain pathway. For further clinical development, it will thus ultimately be important to determine whether systemic delivery of compound 10e may have adverse central nervous system or cardiovascular effects and whether the compound has a better safety profile compared with other blockers such as Z944. Overall, we have identified a new T-type calcium channel blocker with efficacy as an analgesic. Insights gained from the structure-activity relationship of this compound class will help inform the design of additional novel Cav3.2 channel inhibitors.

#### Author contributions

ZP and PS were responsible for the chemistry. FXZ performed the electrophysiology, VMG and SM performed the behavioral analysis. FXZ, VMG, SM, GWZ and YT wrote the manuscript, GWZ and YT designed the study and supervised the

work. Zubaidha Pudukulatham and Fang-Xiong Zhang contribute equally to this work.

### Authors' Note

We synthesized and identified a series of novel piperazine derivatives, tested their effects on Cav3.2 calcium channels, and assessed their *in vivo* effects on inflammatory pain.

### Acknowledgments

We thank Mrs. Lina Chen for cell culture and transfection.

### Declaration of Conflicting Interests

The author(s) declared no potential conflicts of interest with respect to the research, authorship, and/or publication of this article.

### Funding

The author(s) disclosed receipt of the following financial support for the research, authorship, and/or publication of this article: This study was supported by a Foundation Grant from the Canadian Institutes for Health Research to GWZ and the Vi Riddell Child Pain program of the Alberta Children's Hospital Research Institute. ZP and PS thank to Department of Science and Technology (DST), India for INSPIRE fellowship. SM is supported by an Eyes High Postdoctoral Fellowship from the University of Calgary.

### References

1. Simms BA and Zamponi GW. Neuronal voltage-gated calcium channels: structure, function, and dysfunction. *Neuron* 2014; 82: 24–45. DOI: 10.1016/j.neuron.2014.03.016.
2. Zamponi GW, Striessnig J, Koschak A, et al. The physiology, pathology, and pharmacology of voltage-gated calcium channels and their future therapeutic potential. *Pharmacol Rev* 2015; 67: 821–870. DOI: 10.1124/pr.114.009654.
3. Perez-Reyes E. Molecular physiology of low-voltage-activated t-type calcium channels. *Physiol Rev* 2003; 83: 117–161. DOI: 10.1152/physrev.00018.2002.
4. Huguenard JR and Prince DA. A novel T-type current underlies prolonged Ca(2+)-dependent burst firing in GABAergic neurons of rat thalamic reticular nucleus. *J Neurosci* 1992; 12: 3804–3817.
5. Weiss N, Hameed S, Fernandez-Fernandez JM, et al. A Ca(v)3.2/syntaxin-1A signaling complex controls T-type channel activity and low-threshold exocytosis. *J Biol Chem* 2012; 287: 2810–2818. DOI: 10.1074/jbc.M111.290882.
6. Khosravani H and Zamponi GW. Voltage-gated calcium channels and idiopathic generalized epilepsies. *Physiol Rev* 2006; 86: 941–966. DOI: 10.1152/physrev.00002.2006.
7. Heron SE, Khosravani H, Varela D, et al. Extended spectrum of idiopathic generalized epilepsies associated with CACNA1H functional variants. *Ann Neurol* 2007; 62: 560–568. DOI: 10.1002/ana.21169.
8. Bourinet E, Alloui A, Monteil A, et al. Silencing of the Cav3.2 T-type calcium channel gene in sensory neurons demonstrates its major role in nociception. *EMBO J* 2005; 24: 315–324. DOI: 10.1038/sj.emboj.7600515.
9. Marger F, Gelot A, Alloui A, et al. T-type calcium channels contribute to colonic hypersensitivity in a rat model of irritable bowel syndrome. *Proc Natl Acad Sci U S A* 2011; 108: 11268–11273. DOI: 10.1073/pnas.1100869108.
10. Jagodic MM, Pathirathna S, Joksovic PM, et al. Upregulation of the T-type calcium current in small rat sensory neurons after chronic constrictive injury of the sciatic nerve. *J Neurophysiol* 2008; 99: 3151–3156. DOI: 10.1152/jn.01031.2007.
11. Jagodic MM, Pathirathna S, Nelson MT, et al. Cell-specific alterations of T-type calcium current in painful diabetic neuropathy enhance excitability of sensory neurons. *J Neurosci* 2007; 27: 3305–3316. DOI: 10.1523/JNEUROSCI.4866-06.2007.
12. Zamponi GW. Targeting voltage-gated calcium channels in neurological and psychiatric diseases. *Nat Rev Drug Discov* 2016; 15: 19–34. DOI: 10.1038/nrd.2015.5.
13. Bladen C, McDaniel SW, Gadotti VM, et al. Characterization of novel cannabinoid based T-type calcium channel blockers with analgesic effects. *ACS Chem Neurosci* 2015; 6: 277–287. DOI: 10.1021/cn500206a.
14. Bladen C, Gadotti VM, Gunduz MG, et al. 1,4-Dihydropyridine derivatives with T-type calcium channel blocking activity attenuate inflammatory and neuropathic pain. *Pflugers Arch* 2015; 467: 1237–1247. DOI: 10.1007/s00424-014-1566-3.
15. Gadotti VM, You H, Petrov RR, et al. Analgesic effect of a mixed T-type channel inhibitor/CB2 receptor agonist. *Mol Pain* 2013; 9: 32. DOI: 10.1186/1744-8069-9-32.
16. Lee M. Z944: a first in class T-type calcium channel modulator for the treatment of pain. *J Peripher Nerv Syst* 2014; 19(Suppl 2): S11–S12. DOI: 10.1111/jns.12080\_2.
17. Ziegler D, Duan WR, An G, et al. A randomized double-blind, placebo-, and active-controlled study of T-type calcium channel blocker ABT-639 in patients with diabetic peripheral neuropathic pain. *Pain* 2015; 156: 2013–2020. DOI: 10.1097/j.pain.0000000000000263.
18. Guo CC, Tong RB and Li KL. Chloroalkyl piperazine and nitrogen mustard porphyrins: synthesis and anticancer activity. *Bioorg Med Chem* 2004; 12: 2469–2475. DOI: 10.1016/j.bmc.2004.01.045.
19. Ananda Kumar CS, Benaka Prasad SB, Vinaya K, et al. Synthesis and in vitro antiproliferative activity of novel 1-benzhydrylpiperazine derivatives against human cancer cell lines. *Eur J Med Chem* 2009; 44: 1223–1229. DOI: 10.1016/j.ejmech.2008.09.025.
20. Borzenko A, Pajouhesh H, Morrison JL, et al. Modular, efficient synthesis of asymmetrically substituted piperazine scaffolds as potent calcium channel blockers. *Bioorg Med Chem Lett* 2013; 23: 3257–3261. DOI: 10.1016/j.bmcl.2013.03.114.
21. Pajouhesh H, Feng ZP, Zhang L, et al. Structure-activity relationships of trimethoxybenzyl piperazine N-type calcium channel inhibitors. *Bioorg Med Chem Lett* 2012; 22: 4153–4158. DOI: 10.1016/j.bmcl.2012.04.054.

22. Ryckebusch A, Deprez-Poulain R, Maes L, et al. Synthesis and in vitro and in vivo antimalarial activity of N1-(7-chloro-4-quinolyl)-1,4-bis(3-aminopropyl)piperazine derivatives. *J Med Chem* 2003; 46: 542–557. DOI: 10.1021/jm020960r.
23. Choo HY and Chung BJ. 3D QSAR studies on new piperazine derivatives with antihistamine and antibradykinin effects. *Arch Pharm Res* 2000; 23: 324–328.
24. Gillard M, Van Der Perren C, Moguilevsky N, et al. Binding characteristics of cetirizine and levocetirizine to human H(1) histamine receptors: contribution of Lys(191) and Thr(194). *Mol Pharmacol* 2002; 61: 391–399.
25. Cunico W, Gomes CR, Moreth M, et al. Synthesis and antimalarial activity of hydroxyethylpiperazine derivatives. *Eur J Med Chem* 2009; 44: 1363–1368. DOI: 10.1016/j.ejmech.2008.04.009.
26. Dorsey JM, Miranda MG, Cozzi NV, et al. Synthesis and biological evaluation of 2-(4-fluorophenoxy)-2-phenylethyl piperazines as serotonin-selective reuptake inhibitors with a potentially improved adverse reaction profile. *Bioorg Med Chem* 2004; 12: 1483–1491. DOI: 10.1016/j.bmc.2003.12.021.
27. Kimura M, Masuda T, Yamada K, et al. Novel diphenylalkyl piperazine derivatives with dual calcium antagonistic and antioxidative activities. *Bioorg Med Chem Lett* 2002; 12: 1947–1950.
28. Kawasaki N, Miyataka H, Nishiki M, et al. Synthesis of trimethylhydroquinone derivatives as anti-allergic agents with anti-oxidative actions. *Chem Pharm Bull (Tokyo)* 1999; 47: 177–181.
29. McCombie SW, Tagat JR, Vice SF, et al. Piperazine-based CCR5 antagonists as HIV-1 inhibitors. III: synthesis, antiviral and pharmacokinetic profiles of symmetrical heteroaryl carboxamides. *Bioorg Med Chem Lett* 2003; 13: 567–571.
30. Yevich JP, New JS, Smith DW, et al. Synthesis and biological evaluation of 1-(1,2-benzisothiazol-3-yl)- and (1,2-benzisoxazol-3-yl)piperazine derivatives as potential antipsychotic agents. *J Med Chem* 1986; 29: 359–369.
31. Becker OM, Dhanoa DS, Marantz Y, et al. An integrated in silico 3D model-driven discovery of a novel, potent, and selective amidosulfonamide 5-HT1A agonist (PRX-00023) for the treatment of anxiety and depression. *J Med Chem* 2006; 49: 3116–3135. DOI: 10.1021/jm0508641.
32. Mayence A, Vanden Eynde JJ, LeCour L Jr., et al. Piperazine-linked bisbenzamidines: a novel class of antileishmanial agents. *Eur J Med Chem* 2004; 39: 547–553. DOI: 10.1016/j.ejmech.2004.01.009.
33. Foye WO, Lemke TL and Williams DA. *Principles of medicinal chemistry*, 4th ed. Baltimore, MD: Williams & Wilkins, 1995.
34. Gadotti VM and Zamponi GW. Cellular prion protein protects from inflammatory and neuropathic pain. *Mol Pain* 2011; 7: 59. DOI: 10.1186/1744-8069-7-59.
35. Garcia-Caballero A, Gadotti VM, Stemkowski P, et al. The deubiquitinating enzyme USP5 modulates neuropathic and inflammatory pain by enhancing Cav3.2 channel activity. *Neuron* 2014; 83: 1144–1158. DOI: 10.1016/j.neuron.2014.07.036.
36. Gadotti VM, Bladen C, Zhang FX, et al. Analgesic effect of a broad-spectrum dihydropyridine inhibitor of voltage-gated calcium channels. *Pflugers Arch* 2015; 467: 2485–2493. DOI: 10.1007/s00424-015-1725-1.
37. Hunskaar S and Hole K. The formalin test in mice: dissociation between inflammatory and non-inflammatory pain. *Pain* 1987; 30: 103–114.
38. Ferreira J, Campos MM, Pesquero JB, et al. Evidence for the participation of kinins in Freund's adjuvant-induced inflammatory and nociceptive responses in kinin B1 and B2 receptor knockout mice. *Neuropharmacology* 2001; 41: 1006–1012.
39. Waxman SG and Zamponi GW. Regulating excitability of peripheral afferents: emerging ion channel targets. *Nat Neurosci* 2014; 17: 153–163. DOI: 10.1038/nn.3602.
40. Rogawski MA. New evidence supporting a role for T-Type Ca(2+) channels in absence epilepsy and in the action of ethosuximide. *Epilepsy Curr* 2002; 2: 57. DOI: 10.1046/j.1535-7597.2002.00020.x.
41. Tringham E, Powell KL, Cain SM, et al. T-type calcium channel blockers that attenuate thalamic burst firing and suppress absence seizures. *Sci Transl Med* 2012; 4(121): 121ra19. DOI: 10.1126/scitranslmed.3003120.
42. Kraus RL, Li Y, Gregan Y, et al. In vitro characterization of T-type calcium channel antagonist TTA-A2 and in vivo effects on arousal in mice. *J Pharmacol Exp Ther* 2010; 335: 409–417. DOI: 10.1124/jpet.110.171058.
43. Choe W, Messinger RB, Leach E, et al. TTA-P2 is a potent and selective blocker of T-type calcium channels in rat sensory neurons and a novel antinociceptive agent. *Mol Pharmacol* 2011; 80: 900–910. DOI: 10.1124/mol.111.073205.
44. Santi CM, Cayabyab FS, Sutton KG, et al. Differential inhibition of T-type calcium channels by neuroleptics. *J Neurosci* 2002; 22: 396–403.
45. Kuga T, Sadoshima J, Tomoike H, et al. Actions of Ca2+ antagonists on two types of Ca2+ channels in rat aorta smooth muscle cells in primary culture. *Circ Res* 1990; 67: 469–480.